

# Simulation of Bipolar Transistor Degradation at Various Dose Rates and Electrical Modes for High Dose Conditions

Gennady I. Zebrev, Alexander S. Petrov, Rustem G. Useinov, Renat S. Ikhsanov, Viktor N. Ulimov, Vasily S. Anashin, Ilya V. Elushov, Maxim G. Drosdetsky, and Artur M. Galimov

**Abstract**—Radiation response of bipolar devices irradiated under various electrical modes and dose rates at high doses has been studied. A nonlinear numerical model including ELDRS effects and electric field reduction at high doses has been developed and validated. Dose degradation of a bipolar transistor's gain factor at different dose rates and electrical modes has been simulated and explained in a unified way, based on dependence of the charge yield in isolation oxides on dose rates and electric fields. It has been shown that at high doses one needs to use a nonlinear, self-consistent numerical approach, accounting for simultaneous suppression of the oxide electric field induced by trapped charge. Correspondingly, two types of degradation saturation have been revealed: (i) due to simultaneous thermal annealing, and (ii) due to total dose dependent electric field reduction in oxides. The former implies proportionality of the saturation dose and degradation level to dose rate, the latter permits dose rate independent saturation levels of degradation.

**Index Terms**—Annealing, bipolar devices, dose rate effects, ELDRS, modeling, radiation effects in devices, simulation, total dose effects.

## I. INTRODUCTION

THE problem of radiation hardness of bipolar devices has been remained acute [1]. Since the target goals of future space missions require TID levels between 300 and 1000 krad(Si), the effects of these dose levels at low dose rate (LDR) irradiation is of great interest [2]. Despite many years of investigations, all the mechanisms of degradation are still not absolutely clear (especially at different dose rates and high doses), that hinders the further development and application of prediction methods. In spite of a large amount of experimental and theoretical work on Enhanced Low Dose Rate Sensitivity (ELDRS) in bipolar devices, this problem retains actuality. This

effect makes the problem of linear circuit radiation hardness prediction for space application a major one [3]. Another major problem for some space mission is the radiation response of bipolar ICs and transistors under high ionizing doses up to  $\sim 1$  Mrad [4]. Interplay between true dose rate and high dose effects additionally muddle the interpretation of experiments. The aim of this work is to investigate experimentally and theoretically the radiation response of bipolar devices at different dose rates and electric modes including high dose irradiation.

## II. NONLINEAR NUMERICAL MODELING

### A. ELDRS Modeling

Oxides in bipolar devices are intended for isolation and passivation of the underlying silicon and screening of dopants during fabrication. Thicknesses of insulating oxides are typically in the range  $0.2 - 0.8 \mu\text{m}$  [5]. Electric fields in insulating oxides  $E_{ox}$  occur even in the unbiased devices due to differences in work function ( $< 1$  V) between oxides, contacts and silicon bulk materials with different underlying doping. Internal electric fields may also be caused by the occurrence of technological fixed charge in the thick oxides. As a result, the electric field in such oxides turns out to be of order  $\geq 10^4 - 10^5$  V/cm which is at least on 1-2 orders of magnitude lower than in thin gate oxides in MOSFETs.

This circumstance leads to the two important consequences. Firstly, low magnitude of electric fields is a necessary condition of occurrence of the ELDRS effects. Secondly, the low magnitudes of internal electric field imply their high sensitivity to external biases and to the charge trapped near the interface during irradiation. Particularly, a density of trapped charge with magnitude of order  $10^{11} \text{ cm}^{-2}$  is sufficient to significantly lower the initial field even at  $E_{ox} \sim 5 \times 10^4$  V/cm. Therefore, an appreciable reduction of electric fields in bipolar oxides may occur during irradiation especially at high dose levels.

Hjalmarson *et al.* [6] pointed out several bimolecular processes that could be related to ELDRS (or, "reduced high-dose-rate sensitivity"). These are, particularly, (a) free electron–free hole recombination and (b) free electron–trapped hole recombination leading to electron capture that neutralizes a trapped hole. Assuming the Langevin mechanism of recombination, the recombination flux ( $\text{cm}^{-2}\text{s}^{-1}$ ) of the former process can be expressed as

Manuscript received September 20, 2013; revised November 19, 2013; accepted January 24, 2014.

G. I. Zebrev, M. G. Drosdetsky, and A. M. Galimov are with the Department of Micro- and Nanoelectronics, Moscow Engineering Physics Institute (National Research Nuclear University), 115409 Moscow, Russia (e-mail: gizebrev@mephi.ru).

A. S. Petrov, R. G. Useinov, R. S. Ikhsanov, and V. N. Ulimov are with the Research Institute of Scientific Instruments, Lytkarino, 140180 Moscow, Russia.

V. S. Anashin and I. V. Elushov are with the JSC Institute of Space Device Engineering, 111250 Moscow, Russia.

Color versions of one or more of the figures in this paper are available online at <http://ieeexplore.ieee.org>.

Digital Object Identifier 10.1109/TNS.2014.2315672

$$J_r \sim \frac{q(\mu_n + \mu_p)}{\varepsilon_{ox}\varepsilon_0} n p d_{ox},$$

where  $q$  is the electron charge,  $d_{ox}$  is the effective oxide thickness,  $\varepsilon_{ox}$  is the oxide dielectric permittivity,  $\varepsilon_0$  is the vacuum permittivity,  $\mu_p$  ( $\mu_n$ ) is the hole (electron) mobility in  $\text{SiO}_2$  ( $\mu_n \gg \mu_p$ ),  $n$  and  $p$  are the instantaneous densities of the mobile electrons and holes in the oxide

$$n \propto K_g P \frac{d_{ox}}{\mu_n E_{ox}}, \quad p \propto K_g P \frac{d_{ox}}{\mu_p E_{ox}},$$

$P$  is a dose rate,  $K_g \cong 8 \times 10^{12} \text{ cm}^{-3} \text{ rad}^{-1}$  is the radiation constant for  $\text{SiO}_2$ . Normalizing  $J_r$  to the total flux of electron and holes  $J_0 \sim K_g P d_{ox}$  one obtains

$$\frac{J_r}{J_0} \sim \frac{q d_{ox}^2}{\varepsilon_{ox}\varepsilon_0 \mu_p E_{ox}^2} K_g P.$$

This ratio is negligible for all reasonable parameter values due to very small transit times and small product  $n \times p$  of the mobile carrier concentrations. The same reason makes unlikely the mechanism of space charge transport restriction [7], [8], since in this case an instantaneous hole density per unit area should be of order  $10^{11} \text{ cm}^{-2}$  to significantly reduce the internal electric field. Trapped holes are capable of enhancing recombination rates since in quasi-steady state conditions the density of trapped holes  $p_t$  are exponentially larger than the density of mobile holes [6]. Zebrev *et al.* pointed out in [9], that enhanced trap-assisted electron-hole recombination at high dose rates may result in a reduction of the effective charge yield, especially for the thick oxides and low electric fields. Using this idea an analytical self-consistent expression was found for the effective charge yield  $\eta_{eff}$ , limited by recombination between mobile electrons and trapped holes [9], [10]

$$\eta_{eff}(P, T, d_{ox}, E_{ox}) = \eta_G(E_{ox}) \frac{(1 + 4f)^{1/2} - 1}{2f}, \quad (1)$$

where a dimensionless function  $f$  is defined as

$$f(P, T, d_{ox}, E_{ox}) \cong \frac{q d_{ox}^2}{6\varepsilon_{ox}\varepsilon_0 \mu_p E_{ox}^2} \eta_G(E_{ox}) K_g P \exp\left(\frac{\varepsilon_p}{k_B T}\right) \quad (2)$$

$T$  is the irradiation temperature,  $k_B$  is the Boltzmann constant,  $\varepsilon_p$  is the effective energy depth of the hole localized states in the oxide bulk (in [9] it was experimentally found that  $\varepsilon_p \cong 0.39 \text{ eV}$ ),  $\eta_G(E_{ox})$  is the field-dependent geminate recombination function which can be determined experimentally typically at rather high  $E_{ox}$  and normally is interpolated by a monotonically increasing function of local electric field  $E_{ox}$  [11, 12]

$$\eta_G(E_{ox}) = \eta_0 + \frac{E_{ox}/E_0}{1 + E_{ox}/E_0} (1 - \eta_0), \quad (3)$$

where  $\eta_0$  and  $E_0$  are the fitting constants parameterizing a high-field region of experimental dependence. Notice that low-field region has only been investigated to a limited extent.

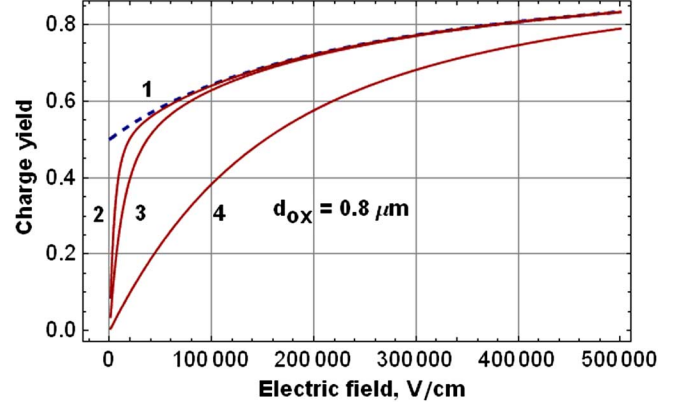


Fig. 1. Simulated dependence of the effective charge yield  $\eta_{eff}$  as functions on the oxide electric fields at different dose rates (1)  $P = 10^{-4} \text{ rad (Si)/s}$  ( $\cong \eta_G$ , dashed line), (2)  $P = 0.1 \text{ rad (Si)/s}$ , (3)  $P = 1.0 \text{ rad (Si)/s}$ , (4)  $P = 10 \text{ rad (Si)/s}$ . Parameters used are  $\eta_0 = 0.5$ ,  $E_0 = 2.5 \times 10^5 \text{ V/cm}$ ,  $\varepsilon_p = 0.39 \text{ eV}$ ,  $\mu_p = 10^{-5} \text{ cm}^2/\text{V} \times \text{s}$ ,  $T = 27^\circ\text{C}$ .

Fig. 1 illustrates that degradation, manifested as dependence of effective charge yield  $\eta_{eff}$ , is reduced for both high dose rates and low electric fields.

Equations (1) and (2) explain also, at least qualitatively, a significant reduction in total dose damage when bipolar integrated circuits are irradiated at low temperature which is observed in [13].

### B. Rate Equations of the Model

Radiation induced degradation can be described by the rate equations set for the variation of the dose-dependent interface recombination trap density  $\Delta N_{RD}$  and the oxide charged trap density  $\Delta N_{ox}$

$$\frac{d\Delta N_{RD}(D)}{dD} = F_{rd} K_g d_{ox} \eta_{eff}(P, E_{ox}) - \frac{\Delta N_{RD}(D)}{P\tau_a} \quad (4a)$$

$$\frac{d\Delta N_{ox}(D)}{dD} = F_{ot} K_g d_{ox} \eta_{eff}(P, E_{ox}) - \frac{\Delta N_{ox}(D)}{P\tau_b} \quad (4b)$$

where  $D$  is total dose,  $\eta_{eff}$  is the effective charge yield,  $F_{rd}$  and  $F_{ot}$  are the dimensionless efficiencies of recombination center and charged oxide trap generation per a radiation-induced electron-hole pair. Notice that a similar equation for  $\Delta N_{RD}$  was written in [10] in a more general form with the time as an independent variable. The proposed equation set describes the quasi-steady-state processes occurring under constant or slowly varying dose rates and temperatures when the effective charge yield can be considered as a function of the current values  $P$  and  $T$  [9]. An explicit dependence of the first term on the r.h.s. of Eqs. (4) on  $P$  is the mathematically formulated hallmark of the true dose rate effects. The thermal annealing temperature-dependent time constants for recombination centers ( $\tau_a$ ) and charged oxide traps ( $\tau_b$ ) are assumed to be specific for different technologies. These rate equations have an instantaneous form, neglecting the temporal delays of degradation buildup due to slow charge transport occurring at low temperatures [14].

Assuming that temperature, dose rate and oxide electric field are constant or weakly varied during irradiation, one gets simple

linear equations. In this case, assuming  $\Delta N_{RD}(0) = 0$ , the analytical solution of Eq. (4a) has an exact form [10]

$$\Delta N_{RD}(D) = F_{rd} K_g d_{ox} \eta_{eff}(P, E_{ox}) P \tau_a \left( 1 - \exp \left( -\frac{D}{P \tau_a} \right) \right) \quad (5)$$

where the saturation level degradation depends generally on dose rate, irradiation temperature, and electric field.

The input base current, or the radiation-induced change in the inverse current gain  $\Delta h_{21}^{-1}$  are normally measured in the experiments. The latter is proportional to  $\Delta N_{RD}$  and can be written using a simple model as

$$\Delta h_{21}^{-1} = \frac{A_S}{A_E} \frac{\sigma_r v_t W_B}{D_B} \Delta N_{RD}, \quad (6)$$

where  $A_S$  is the area of the base-oxide interface,  $A_E$  is the area of the emitter-base junction,  $D_B$  is the diffusivity of minority carriers in the base,  $W_B$  is the base width,  $v_t$  is the carrier's thermal velocity ( $\sim 10^7$  cm/s),  $\sigma_r$  ( $\sim 10^{-15} - 10^{-16}$  cm<sup>2</sup>, chap. 4 of [15]) is the carrier's capture cross-section for the energy levels located near the Si midgap.

### C. Nonlinear Effects at High Doses

The electric field in the oxide for sufficiently large total doses becomes a decreasing function of dose due to screening of initial  $E_{ox}$  by the charged defects trapped near the interface Si – SiO<sub>2</sub>. This makes it necessary to use a simplified electrostatic equation which couples solutions of Eqs. 4(a) and 4(b)

$$E_{ox}(D) = E_{ox0} - \frac{q \Delta N_{ox}(D)}{\varepsilon_{ox} \varepsilon_0}, \quad (7)$$

where  $E_{ox0}$  is the built-in electric field in the oxide before irradiation. Due to nonlinearity of the rate equations a self-consistent solution of Eqs. (4) and (7) can only be obtained numerically. Charge trapping efficiency  $F_{ot}$  is a fitting parameter chosen in such a way to describe the electric field reduction under long-term irradiation.

## III. MODEL VALIDATION

### A. Experiment Conditions

We have irradiated four sets of bipolar devices each consisting of 10 samples of NPN and PNP transistors using a Cobalt-60 source at room temperature at dose rates 0.015 rad(Si)/s and 50 rad(Si)/s. Experimental results are presented in Figs. 2–3 as the ensemble average with the sample-to-sample scatter less than 10%.

Electrical modes during irradiation are presented in Table I. The transistor gain factor of  $h_{21}$  was measured during irradiation at (1) no bias conditions; (2) low input base current (corresponding to gain  $h_{21} \sim 150$ ,  $I_C \sim 20$   $\mu$ A); (3) high input current ( $h_{21} \sim 250$ ,  $I_C \sim 8$  mA). We have also investigated a fixed-output voltage regulator National Semiconductor LP2985 under the same conditions.

### B. Model Validation

In Figs. 2(a) and 3 the dose dependencies of  $h_{21}^{-1}$  for NPN and PNP transistors at the dose rates 0.015 and 50 rad(Si)/s are shown.

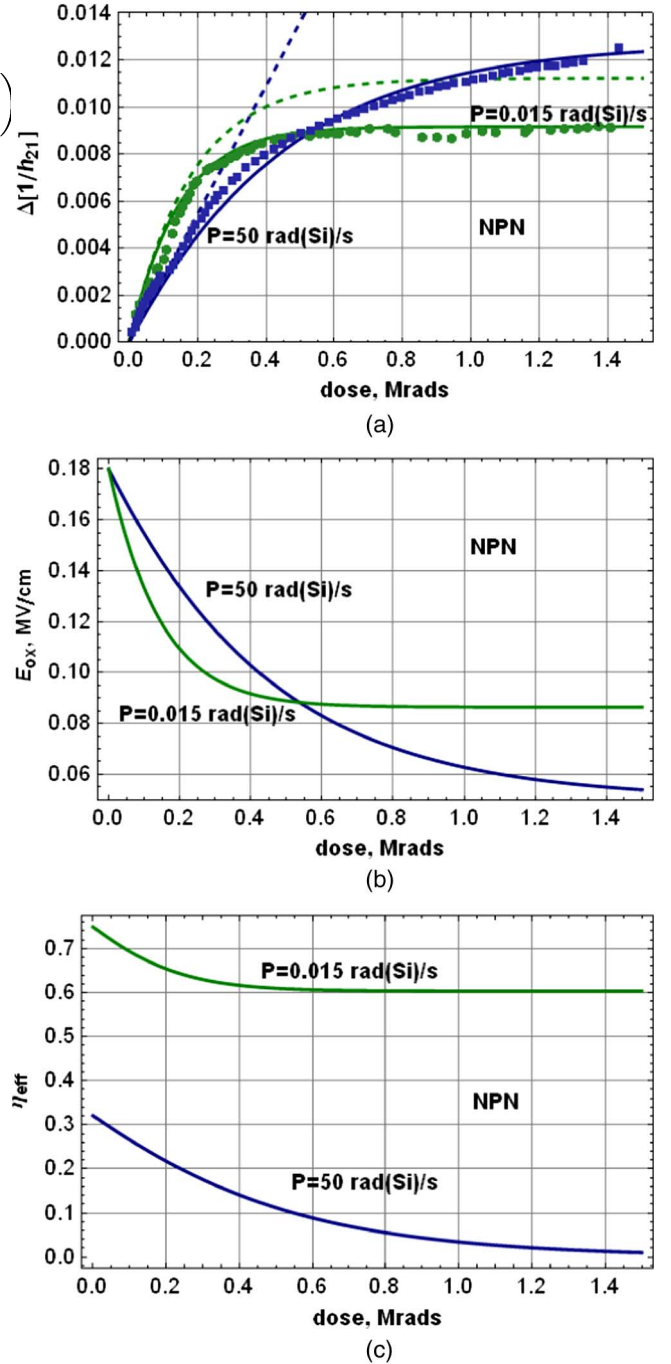


Fig. 2. Comparison between experimental (points) and simulated (lines) dose dependencies of the inverse current gain for NPN bipolar transistors (a) and simulated dose dependencies of the oxide electric field (b) and the effective charge yield (c) at different dose rates. Dashed lines correspond to linear response neglecting the electric field reduction at high doses. Fitted parameters:  $F_{rd} = 1.36 \times 10^{-2}$ ;  $\tau_a = 1.2 \times 10^7$  s;  $E_0 = 1.8 \times 10^5$  V/cm;  $E_{ox0} = 1.3 \times 10^5$  V/cm;  $F_{ot} = 4.6 \times 10^{-3}$ .

Results of numerical simulations with Eqs. (4) and (7) are also presented Figs. 2(a) and 3. Fig. 2(a) shows that a neglect of the non-linear field effect leads to only a slight overestimation of degradation under low dose rate, and is incapable to describe saturation at high dose rate condition.

All simulations were performed for  $d_{ox} = 0.8$   $\mu$ m;  $\eta_0 = 0.5$ ;  $T = 27^\circ\text{C}$ ,  $\varepsilon_p = 0.39$  eV [9];  $\mu_p = 10^{-5}$  cm<sup>2</sup>/V  $\times$  s,

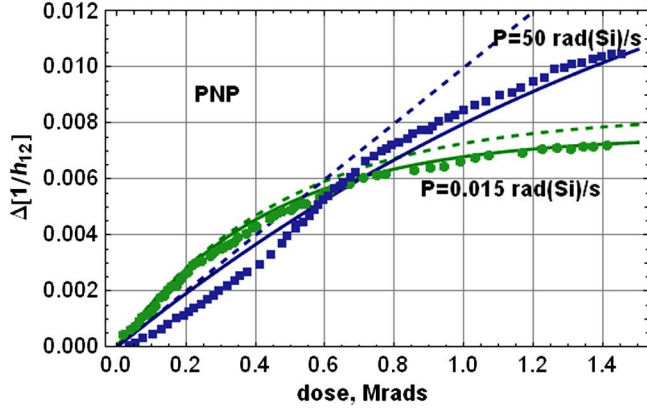


Fig. 3. Comparison between experimental (points) and simulated (lines) dependencies for PNP bipolar transistors at the two dose rates 50 rad(Si)/s and 0.015 rad(Si)/s. Dashed lines correspond to linear response neglecting the electric field reduction at high doses. Fitted parameters:  $F_{rd} = 3.55 \times 10^{-3}$ ;  $\tau_a = 3.6 \times 10^7$  s;  $E_0 = 2.5 \times 10^5$  V/cm;  $E_{ox0} = 2.0 \times 10^5$  V/cm;  $F_{ot} = 1.3 \times 10^{-3}$ .

TABLE I  
ELECTRICAL MODES DURING IRRADIATION

Set number	NPN-transistors	PNP-transistors
1	Passive, at open pins	Passive, at open pins
2	$V_{CE} = 15$ V, $I_B = 0.1$ $\mu$ A	$V_{CE} = -15$ V, $I_B = 0.1$ $\mu$ A
3	$V_{CE} = 10$ V, $I_B = 32$ $\mu$ A	$V_{CE} = -10$ V, $I_B = 32$ $\mu$ A

$\sigma_r = 1 \times 10^{-15}$  cm<sup>2</sup>,  $D_B = 10$  cm<sup>2</sup>/s,  $A_S/A_E = 1/1$ ,  $W_B = 0.1$   $\mu$ m. Only the  $F_{rd}$ ,  $F_{ot}$ ,  $E_{ox0}$ ,  $E_0$  and  $\tau_a$  were fitted parameters in numerical calculations. For the sake of simplicity we assumed here  $\tau_a = \tau_b$ . The slopes of the linear parts of dose curves are determined by  $F_{rd}$  and by the effective charge yield  $\eta_{eff}$  at the initial electric field  $E_{ox0}$  in Eq. 4(a). Fitted parameters presented in the figures have rather reasonable numerical values  $F_{rd}$ ,  $F_{ot} \ll 1$  despite many uncertainties in the choice of constant numerical parameters.

We argue that the degradation saturation observed at low dose rate case ( $P = 0.015$  rad(Si)/s) is mainly caused by the thermal annealing of the recombination centers dominating at large irradiation time scales. As can be seen in Figs. 2(a) and 3, the saturation doses  $D_{SAT}$  under low-dose rate irradiation are of order 0.3-0.7 Mrads. Then, the annealing time constants can be estimated as  $\tau_a = D_{SAT}/P \geq 10^7$  s.

For a dose rate of 50 rad(Si)/s, the expected saturation doses  $D_{SAT} = P\tau_a$  for such  $\tau_a$  become of magnitude of order of hundreds Mrads, when the linear approximation is not valid and internal built-in electric fields become fully suppressed by the trapped charge. We argue, therefore, that in contrast to the low dose rate (0.015 rad(Si)/s) case, the weakly pronounced saturation at 50 rad(Si)/s is mainly caused by reduction of the oxide electric field due to screening by the charge trapped at high doses. This statement is illustrated by numerical simulation results for the NPN BJT in Fig. 2(b) and 2(c). The significance of simultaneous annealing, described by the second terms

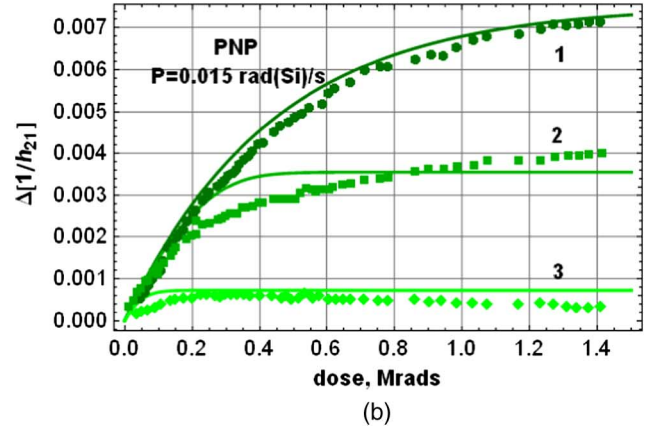
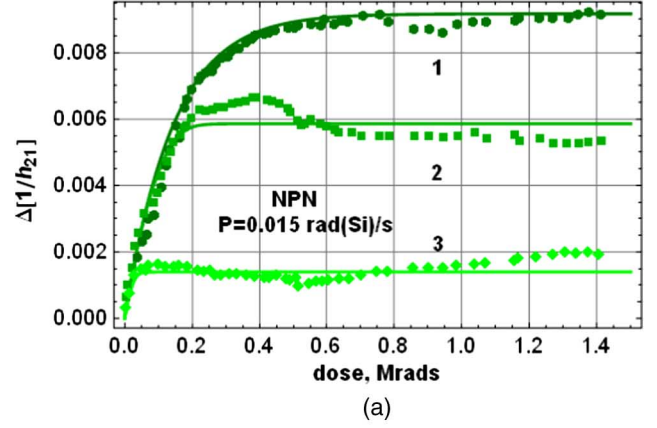


Fig. 4. Comparison between experimental (points) and simulated (lines) dependencies for of NPN (a) and PNP (b) bipolar transistors at various electric modes (see Table I). The curves 1 in Fig. 4(a) and 4(b) are the same as in Figs. 2(a) and 3 at  $P = 0.015$  rad(Si)/s. All fitted parameters for NPN and PNP samples are the same as in Fig. 2 excepting  $E_{ox0}(\text{NPN}, 1) = 1.3 \times 10^5$  V/cm;  $E_{ox0}(\text{NPN}, 2) = 6.5 \times 10^4$  V/cm;  $E_{ox0}(\text{NPN}, 3) = 1.5 \times 10^4$  V/cm;  $E_{ox0}(\text{PNP}, 1) = 2 \times 10^5$  V/cm;  $E_{ox0}(\text{PNP}, 2) = 4.5 \times 10^4$  V/cm;  $E_{ox0}(\text{PNP}, 3) = 0.9 \times 10^4$  V/cm.

on the r.h.s. of Eqs. (4), decrease as  $P\tau_a$  increases. In absence of appreciate thermal annealing the electric field and the effective charge yield at 50 rad(Si)/s lower as functions of dose causing the degradation saturation due to electric field reduction.

### C. Electric Mode Influence

The same types of devices were studied under low dose rate (0.015 rad(Si)/s) irradiation at the different electric conditions. Fig. 4(a) and 4(b) show experimental results measured for these three electric regimes of irradiation (see Table I) and simulation results with fitted parameters. Since radiation degradation coupled with the field-dependent charge yield is an increasing function of electric field, it seems to be sensitive to electric bias during irradiation. Forward emitter-base bias  $V_{BE}$  decreases the lateral oxide electric field above the emitter-base junction thus reducing the charge yield and degradation.

One can see that in Fig. 4(a) and 4(b) the most intensive degradation of  $h_{21}^{-1}$  with total dose occurs in the no bias case, i.e. for maximum magnitudes of electric fields above the emitter-base junction. As expected the low dose rate irradiation in the unbiased condition is the worst case as it has been shown for many sensitive electrical parameters (e.g., input bias



current, output source/sink current, and reference or output voltage) [16], [17], [18], [19].

The lowest degradation occurs at maximal base current i.e. at highest forward bias of emitter junction and lowest electric field above the emitter junction. We simulate different electric conditions in Fig. 4 fitting only initial electric fields  $E_{ox0}$  for each regime.

Remarkably, in the linear response approximation the saturation of degradation arises due to quasi-steady compensation of buildup and annealing processes, and both the degradation saturation dose and saturation level in Eq. (5) turn out to be necessarily proportional to the dose rate in this case. Analysis shows that the simultaneous Radiation-Induced Charge Neutralization (RICN) annealing [20], [9] leads to the same saturation doses and different saturation levels at high dose rates (HDR) and low dose rates (LDR).

That is generally wrong for the nonlinear response when degradation saturation may occur due to reduction of internal electric field and charge yield.

Such situation may arise for devices with relatively low electric field  $E_{ox}$  and/or large annealing time constant  $\tau_a$ . In this case the degradation saturation level may not depend on dose rate. This behavior has been often observed experimentally (see, for example, [21]). Simulation results in Fig. 5(a) illustrate this point. Simulated curves are in good agreement with experimental data for the LM139 irradiated with all pins grounded as shown in Fig. 9 of [21].

Simulation results for low  $E_{ox0}$  does not practically depend on the annealing time constant suggesting thereby the saturation due to electric field reduction (see, also, Fig. 5(b)). In contrast to the annealing induced saturation, the electric field reduction mechanism allows the dose rate independent levels of degradation saturation.

Importance of different saturation mechanisms depends mainly on magnitudes of parameters  $F_{ot}$ ,  $F_{rd}$ ,  $E_{ox0}$  and the temperature-dependent product  $P\tau_a$ . For large enough  $P\tau_a$  and  $F_{ot}$  the annealing term in the rate equation can be neglected and degradation saturates due to electric field reduction. In opposite case of low  $F_{ot}$  and  $P\tau_a$  the simultaneous annealing dominates, yielding the dose rate dependent saturation levels. Unfortunately, the fitting procedure does not provide a unique set of fitted parameters at restricted experimental data. Additional data (e.g. measurements at different temperatures, etc.) are generally required to improve accuracy and uniqueness of fitting.

#### D. Additional Experiment

Qualitatively similar interplay between LDR and HDR irradiation at rather high dose may take place in some complex circuits. For example, Fig. 6 shows measured dose behavior of the output voltage for fixed-output voltage regulator National Semiconductor LP2985. As in discrete bipolar devices the LDR irradiation leads to lesser parametrical failure dose compared to a HDR case due to ELDRS effects. All the curves do not manifest any saturation at doses up 120 krad (Si), and what is more, the

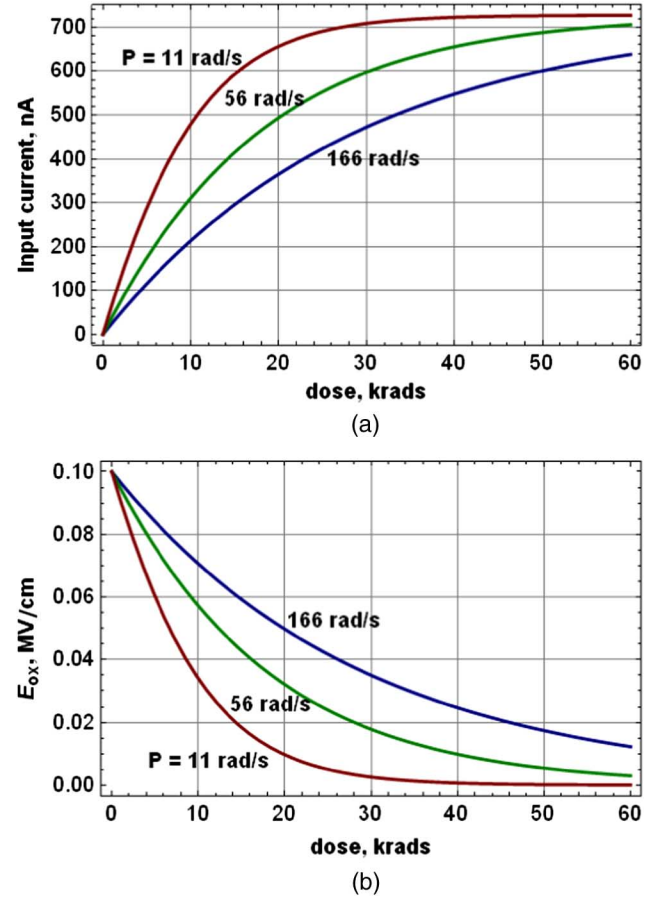


Fig. 5. Simulated dose dependencies of input current (a) and oxide electric field (b) of bipolar device at different dose rates (in rad (SiO<sub>2</sub>)/s). Fitted parameters:  $E_0 = 2.5 \times 10^5$  V/cm;  $E_{ox0} = 0.4 \times 10^4$  V/cm;  $F_{rd} = 3.8 \times 10^{-2}$ ,  $F_{ot} = 6.8 \times 10^{-2}$ .

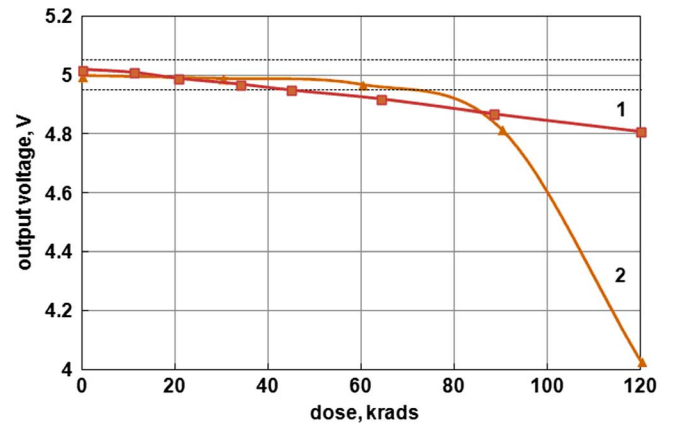


Fig. 6. Output voltage of a regulator National Semiconductor LP2985 measured as functions of dose at different dose rates (1) 0.014 rad(Si)/s (failure dose  $\sim$  45 krad); (2) 51.7 rad(Si)/s (failure dose  $\sim$  70 krad(Si)). Two dashed lines show the margins of parametric failure.

output voltage under HDR irradiation exhibits drastic enhancement of degradation at approximately 80 krad.

This behavior of degradation at high dose rates may be only explained by nonlinear internal reaction of complex circuit. Such effects are not yet contained of course in our simulation scheme.

## IV. CONCLUSION

The main essence of this work is an attempt to quantitatively and qualitatively describe the radiation-induced behavior of bipolar transistors irradiated with high doses based on the charge yield dependence on dose rate and electric field in the bipolar oxides. The computational scheme and experimental results presented in this paper demonstrate the possibility of numerically describing in a self-consistent way the processes of radiation-induced degradation in bipolar devices including the ELDRS effects, simultaneous annealing, electric field suppression in the oxides at high doses. The presented model neglects many important aspects of the problem such as a delay in hole transport and recombination center buildup especially at low temperatures [14]; the impact of hydrogenic species on temporal behavior of degradation [22], circuit effects [23], etc. Some of these aspects can, at least partially, be incorporated into the mathematical structure of the model. For example, a solution of full transport equation with spatial gradients for holes (as can be done in original paper [9]) simultaneously with solution of the rate equations for other species [24], [25], [26] would allow us to get a more complete description of degradation at different conditions. In practice, such necessity is required only for simultaneous description of a very wide set of experimental data obtained at different temperatures, hydrogen ambients, etc.

## ACKNOWLEDGMENT

The authors would like to thank the reviewers of this paper for their valuable feedback. One of the authors (G. I. Z.) thanks I. P. Lopyrev for technical support.

## REFERENCES

- [1] K. F. Galloway, R. L. Pease, R. D. Schrimpf, and D. W. Emily, "From displacement damage to ELDRS: Fifty years of bipolar transistor radiation effects at the NSREC," *IEEE Trans. Nucl. Sci.*, vol. 60, no. 3, pp. 1731–1739, Jun. 2013.
- [2] L. Scheick, A. H. Johnston, P. Adell, F. Irom, and S. McClure, "Total ionizing dose (TID) and displacement damage (DD) effects in integrated circuits," JAXA Special Publication JAXA-SP-12-008E, 2012, p. 166.
- [3] R. L. Pease, R. D. Schrimpf, and D. M. Fleetwood, "ELDRS in bipolar linear circuits: A review," *IEEE Trans. Nucl. Sci.*, vol. 56, no. 4, pp. 1894–1908, Aug. 2009.
- [4] R. D. Harris, S. S. McClure, B. G. Rax, D. O. Thornbourn, A. J. Kenna, K. B. Clark, and T.-Y. Yan, "ELDRS characterization for a very high dose mission," in *Proc. IEEE Radiation Effects Data Workshop*, 2010.
- [5] A. H. Johnston, R. T. Swimm, and D. O. Thornbourn, "Total dose effects on bipolar integrated circuits at low temperature," *IEEE Trans. Nucl. Sci.*, vol. 59, no. 6, pp. 2995–3003, Dec. 2012.
- [6] H. P. Hjalmarson, R. L. Pease, S. C. Witzak, M. R. Shaneyfelt, J. R. Schwank, A. H. Edwards, C. E. Embree, and T. R. Mattsson, "Mechanisms for radiation dose-rate sensitivity of bipolar transistors," *IEEE Trans. Nucl. Sci.*, vol. 50, no. 6, pp. 1901–1909, Dec. 2003.
- [7] D. M. Fleetwood, L. C. Riewe, J. R. Schwank, S. C. Witzak, and R. D. Schrimpf, "Radiation effects at low electric fields in thermal, SIMOX, and bipolar-base oxides," *IEEE Trans. Nucl. Sci.*, vol. 43, no. 6, pp. 2573–2546, Dec. 1996.
- [8] S. C. Witzak, R. C. Lacoe, D. C. Mayer, D. M. Fleetwood, R. D. Schrimpf, and K. F. Galloway, "Space charge limited degradation of bipolar oxides at low electric fields," *IEEE Trans. Nucl. Sci.*, vol. 45, no. 6, pp. 2339–2351, Dec. 1998.
- [9] G. I. Zebrev, D. Y. Pavlov, V. S. Pershenkov, A. Y. Nikiforov, A. V. Sogoyan, D. V. Boychenko, V. N. Ulimov, and V. V. Emelianov, "Radiation response of bipolar transistors at irradiation temperatures and electric biases: Modeling and experiment," *IEEE Trans. Nucl. Sci.*, vol. 53, no. 4, pp. 1981–1987, Aug. 2006.
- [10] G. I. Zebrev and M. S. Gorbunov, "Modeling of radiation-induced leakage and low dose-rate effects in thick edge isolation of modern MOSFETs," *IEEE Trans. Nucl. Sci.*, vol. 56, no. 4, pp. 2230–2236, Aug. 2009.
- [11] M. R. Shaneyfelt, D. M. Fleetwood, J. R. Schwank, and K. L. Hughes, "Charge yield for cobalt-60 and 10-keV x-ray irradiations of MOS devices," *IEEE Trans. Nucl. Sci.*, vol. 38, no. 6, pp. 1187–1194, Dec. 1991.
- [12] C. Brisset, V. Ferlet-Cavrois, O. Flament, O. Musseau, J. L. Leray, J. L. Pelloie, R. Escoffier, A. Michez, C. Cirba, and G. Bordure, "Two-dimensional simulation of total dose effects on NMOSFET with lateral parasitic transistor," *IEEE Trans. Nucl. Sci.*, vol. 43, no. 6, pp. 2651–2658, Dec. 1996.
- [13] A. H. Johnston, R. T. Swimm, and D. O. Thornbourn, "Charge yield at low electric fields: Considerations for bipolar integrated circuits," *IEEE Trans. Nucl. Sci.*, vol. 60, no. 6, pp. 4488–4497, Dec. 2013.
- [14] A. H. Johnston, R. T. Swimm, R. D. Harris, and D. O. Thornbourn, "Dose rate effects on linear bipolar transistors," *IEEE Trans. Nucl. Sci.*, vol. 58, no. 6, pp. 2816–2823, Dec. 2011.
- [15] S. M. Sze and K. K. Ng, *Physics of Semiconductor Devices*, 3rd ed. Hoboken, NJ, USA: Wiley-InterScience, 2007.
- [16] R. L. Pease, S. McClure, J. Gorelik, and S. C. Witzak, "Enhanced low-dose-rate sensitivity of a low-dropout voltage regulator," *IEEE Trans. Nucl. Sci.*, vol. 45, no. 6, pp. 2571–2576, Dec. 1998.
- [17] S. S. McClure, J. L. Gorelik, R. Pease, and A. H. Johnston, "Dose rate and bias dependency of total dose sensitivity of low dropout voltage regulators," in *Proc. IEEE Radiation Effects Data Workshop Rec.*, 2000, pp. 100–105.
- [18] P. Adell, "The rule of total ionizing dose evaluations qualifying electronics for a space mission," presented at the Radiation and its Effects on Components and Systems Conf., 2011, Short Course.
- [19] V. S. Pershenkov, V. B. Maslov, S. V. Cherepko, I. N. Shvetzov-Shilovsky, V. V. Belyakov, A. V. Sogoyan, V. I. Rusanovsky, V. N. Ulimov, and V. V. Emelianov, "The effect of emitter junction bias on the low dose-rate radiation response of bipolar devices," *IEEE Trans. Nucl. Sci.*, vol. 44, no. 6, pp. 1840–1848, Dec. 1997.
- [20] D. M. Fleetwood, "Radiation-induced charge neutralization and interface-trap buildup in MOS devices," *J. Appl. Phys.*, vol. 67, p. 580, 1990.
- [21] J. Boch, Y. G. Velo, F. Saigné, N. J.-H. Roche, R. D. Schrimpf, J.-R. Vaillat, L. Dusseau, C. Chatry, E. Lorfevre, R. Ecoffet, and A. D. Touboul, "The use of a dose-rate switching technique to characterize bipolar devices," *IEEE Trans. Nucl. Sci.*, vol. 56, no. 6, pp. 3347–3353, Dec. 2009.
- [22] R. L. Pease, P. C. Adell, B. G. Rax, X. J. Chen, H. J. Barnaby, K. E. Holbert, and H. P. Hjalmarson, "The effect of hydrogen on the ELDRS in bipolar linear circuits," *IEEE Trans. Nucl. Sci.*, vol. 55, no. 6, pp. 3169–3173, Dec. 2008.
- [23] A. H. Johnston, B. G. Rax, and D. Thornbourn, "Total dose effects in op-amps with compensated input stages," in *Proc. Radiation and its Effects on Components and Systems Conf.*, 2007, pp. 1–8.
- [24] N. L. Rowsey, M. E. Law, R. D. Schrimpf, D. M. Fleetwood, B. R. Tuttle, and S. T. Pantelides, "Mechanisms separating time-dependent and true dose-rate effects in irradiated bipolar oxides," *IEEE Trans. Nucl. Sci.*, vol. 59, no. 6, pp. 3069–3076, Dec. 2012.
- [25] I. S. Esqueda, H. J. Barnaby, P. C. Adell, B. G. Rax, H. P. Hjalmarson, M. L. McLain, and R. L. Pease, "Modeling low dose rate effects in shallow trench isolation oxides," *IEEE Trans. Nucl. Sci.*, vol. 58, no. 6, pp. 2945–2952, Dec. 2011.
- [26] I. S. Esqueda, H. J. Barnaby, and P. C. Adell, "Modeling the effects of hydrogen on the mechanisms of dose rate sensitivity," *IEEE Trans. Nucl. Sci.*, vol. 59, no. 4, pp. 701–706, Aug. 2012.